622

Fermilab Library
0 1160 0038889 6

MIDWESTERN UNIVERSITIES RESEARCH ASSOCIATION

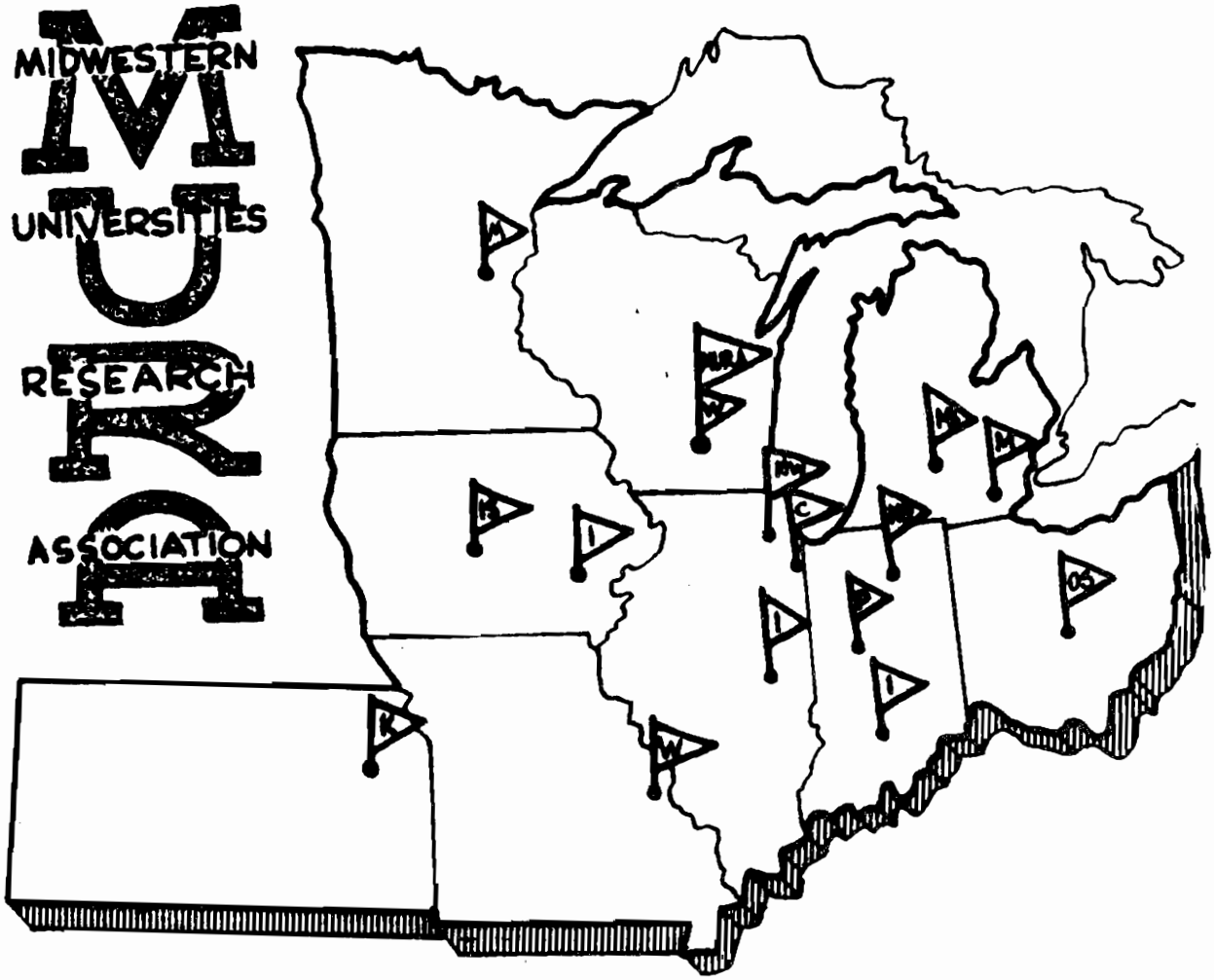

PROTON LINEAR ACCELERATOR CAVITY CALCULATIONS

Terry W. Edwards

REPORT **NUMBER** 622

MURA-622
UC-28, Particle Accelerators and
High Voltage Machines
TID-4500 (16th Edition)

MIDWESTERN UNIVERSITIES RESEARCH ASSOCIATION*

2203 University Avenue, Madison, Wisconsin

PROTON LINEAR ACCELERATOR CAVITY CALCULATIONS

June 15, 1961

Terry W. Edwards

ABSTRACT

The calculation of electromagnetic eigenvectors and eigenvalues in linear accelerator type cavities containing drift-tubes, whose meridian-plane cross sections are piece-wise simply describable, can be accomplished by solving finite difference approximations to the wave equation. The resulting eigenfunctions and eigenvalues allow quantitative determination of particle dynamic and electromagnetic phenomena occuring within an operating linear accelerator. The development and method of use of these finite difference relationships are examined. Preliminary results computed from these relationships agree with known information. Computer programs have been written for cavities whose shapes are applicable to low energy proton-linear accelerators.

*AEC Research and Development Report. Research supported by the U.S. Atomic Energy Commission, Contract No. AT(11-1)-384.

TABLE OF CONTENTS

I. Introduction 1

II. Survey of Previous Calculations 3

III. Field Calculations for Cavities of Revolution 5

A. General Relationships 5

B. Exact Solutions of the Wave Equation 10

C. Variational Principle Approach to Approximate Solutions of the Wave Equation 11

D. Approximate Solutions of the Wave Equation for Cavities Containing Square Cornered Drift-Tubes 15

E. Approximate Solutions of the Wave Equation for Cavities Containing Round and Elliptical Cornered Drift-Tubes 18

IV. Iterative Solution of Finite-Difference Equations 24

A. General Features 24

B. Mesh Refinement 25

C. Eigenvalue Calculation 27

D. Interpolation Between Meshes 29

E. Normalization 32

V. Associated Electromagnetic and Particle Dynamic Quantities 35

VI. Computation Programs 38

A. Present Status 38

B. Comparison of Results Obtained With Known Data 38

C. Future Aims and Additions 38

VII. Conclusion 40

References 41

I. INTRODUCTION

In order to substantially increase the final energy of proton linear accelerators above the present levels of 50-70 Mev, it seems mandatory that close attention be paid to the relative merits of the proposed configuration. Such careful attention will assist with the selection of the configuration which best combines high duty cycle, high intensity, low power dissipation, and simplicity of construction.

To date, many of the calculations done in connection with linear accelerators have been done in a semi-rigorous analytic fashion; only recently has use of large, modern, high-speed, digital computers been made. The primary aim of the present endeavor is to adapt to and solve via digital computers some of the problems associated with linear accelerators.

The finite mesh approach to the calculation of eigenfunctions and eigenvalues, as developed herein, has the property that the only error, that due to the finite difference approximation, tends to disappear as the mesh is refined by including more mesh points. This fact coupled with the immense data handling capabilities of digital computers indicates the desirability and practicability of this approach.

Analysis directed toward computer calculations of eigenfunctions and eigenvalues of rotationally symmetric geometries, whose meridian plane cross-sections are bounded by piece-wise combinations of straight lines, circles, and ellipses, are included herein, as are considerations of some of the pertinent electromagnetic and particle dynamic phenomena occuring within operating linear accelerators.

II. SURVEY OF PREVIOUS CALCULATIONS

Many of the electromagnetic field calculations previously attempted in connection with the design of linear accelerators have been either of an approximate or empirical nature. Recently, however, techniques whose errors due to approximations vanish under certain conditions have been attempted; in fact, the present endeavor attempts to enumerate a few of these techniques.

Some of the earliest calculations carried out with respect to rotationally symmetric resonant cavities were those of Hansen[1] and Hahn.[2] Parameters pertaining to electron linear accelerators, in which disk-loaded wave quides are suitable accelerating cavities, have been calculated by Brillouin,[3,4] Chu and Hansen,[5] Walkinshaw,[6,7] and Bell.[7,8]

Approximate calculations pertaining to proton linear accelerators, in which drift-tube loaded cavities must be used, are to be found in the works of Walkinshaw, et al.,[9] Wilkins,[10] Christofilos,[11] and Taylor.[12] The latter reference contains an empirically based consideration of drift tubes whose corners are rounded with radii of non-vanishing size.

The principal approximation inherent in most of the above mentioned calculations involve assumptions concerning the field components (the unknown quantities)

and about the matching conditions to be employed at the intersection of the two regions in which the fields are to be expanded in sets of orthogonal polynomials. Furthermore, application of these methods to cavities whose meridian-plane boundaries are not rectilinear is difficult if not impossible. Accordingly, the present endeavor was undertaken to present a more satisfactory treatment of the problem.

III. FIELD CALCULATIONS FOR CAVITIES OF REVOLUTION

A. General Relationships

Derivable from Maxwell's electromagnetic field equations for non-conducting, charge free media,

$$\nabla \times \bar{E} = -\frac{\partial \bar{B}}{\partial t} \tag{3.1a}$$

$$\nabla \times \bar{H} = \frac{\partial \bar{D}}{\partial t} \tag{3.1b}$$

$$\nabla \cdot \bar{D} = 0 \tag{3.1c}$$

$$\nabla \cdot \bar{B} = 0 \ , \tag{3.1d}$$

are the vector wave equations

$$-\nabla \times \nabla \times \bar{E} + \nabla(\nabla \cdot \bar{E}) = \nabla^2 \bar{E} = \mu \epsilon \frac{\partial^2 \bar{E}}{\partial t^2} \tag{3.2}$$

$$-\nabla \times \nabla \times \bar{H} + \nabla(\nabla \cdot \bar{H}) = \nabla^2 \bar{H} = \mu \epsilon \frac{\partial^2 \bar{H}}{\partial t^2} \ . \tag{3.3}$$

If the $\bar{E}$ or $\bar{H}$ wave impinges upon a perfectly conducting surface, the boundary condition which must be obeyed is

$$\bar{n} \times \bar{E} = 0 \ . \tag{3.4}$$

It is easily shown that in rotationally symmetric cavities, two possible azimuthally independent mode types exist. The

choice of which mode type to consider is dependent upon the necessity of having a non-zero component of $\bar{E}$ in the axial direction so as to permit acceleration of particles.

Let both $\bar{E}$ and $\bar{H}$ be divided into two components, one in the azimuthal direction, and one in the meridian plane, such that

$$\bar{E} = \left[\bar{E}_\varphi + \bar{E}_M\right] e^{-i\omega t} \tag{3.5}$$

$$\bar{H} = \left[\bar{H}_\varphi + \bar{H}_M\right] e^{-i\omega t} \tag{3.6}$$

Similarly, dividing the $\bar{\nabla}\times$ operator into two components, one in the azimuthal direction, the other in the meridian plane, Maxwell's equations (3.1a) and (3.1b) demand that

$$(\bar{\nabla}_\varphi \times \bar{E}_\varphi) + (\bar{\nabla}_\varphi \times \bar{E}_M) + (\bar{\nabla}_M \times \bar{E}_\varphi) + (\bar{\nabla}_M \times \bar{E}_M) = i\omega\mu \bar{H}_\varphi + i\omega\mu \bar{H}_M , \tag{3.7}$$

$$(\bar{\nabla}_\varphi \times \bar{H}_\varphi) + (\bar{\nabla}_\varphi \times \bar{H}_M) + (\bar{\nabla}_M \times \bar{H}_\varphi) + (\bar{\nabla}_M \times \bar{H}_M) = -i\omega\epsilon \bar{E}_\varphi - i\omega\epsilon \bar{E}_M . \tag{3.8}$$

Noting that $(\bar{\nabla}_\varphi \times \bar{E}_\varphi) = 0$ and $(\bar{\nabla}_\varphi \times \bar{H}_\varphi) = 0$, equations (3.7) and (3.8) yield, for the meridian plane components,

$$(\bar{\nabla}_M \times \bar{E}_\varphi) + (\bar{\nabla}_M \times \bar{E}_M) = i\omega\mu \bar{H}_M \ , \tag{3.9}$$

$$(\bar{\nabla}_M \times \bar{H}_\varphi) + (\nabla_M \times \bar{H}_M) = -i\omega\epsilon \bar{E}_M \ . \tag{3.10}$$

Now, substituting each of equations (3.10) and (3.9) into the other for $\bar{E}_m$ and $\bar{H}_m$, respectively, it follows that

$$-i\omega\epsilon(\bar{\nabla}_M \times \bar{E}_\varphi) + \bar{\nabla}_M \times (\bar{\nabla}_M \times \bar{H}_\varphi) + \bar{\nabla}_M \times (\bar{\nabla}_M \times \bar{H}_M) = \omega^2\mu\epsilon \bar{H}_M \ , \tag{3.11}$$

$$i\omega\mu(\bar{\nabla}_M \times \bar{H}_\varphi) + \bar{\nabla}_M \times (\bar{\nabla}_M \times \bar{E}_\varphi) + \bar{\nabla}_M \times (\bar{\nabla}_M \times \bar{E}_M) = \omega^2\mu\epsilon \bar{E}_M \ . \tag{3.12}$$

Also noting that, for azimuthally independent modes, the terms $\bar{\nabla}_M \times (\bar{\nabla}_M \times \bar{H}_M)$ and $\bar{\nabla}_M \times (\bar{\nabla}_M \times \bar{E}_M)$ vanish, there results

$$-i\omega\epsilon(\bar{\nabla}_M \times \bar{E}_\varphi) + \bar{\nabla}_M \times (\bar{\nabla}_M \times \bar{H}_\varphi) = \omega^2\mu\epsilon \bar{H}_M \ , \tag{3.13}$$

$$i\omega\mu(\bar{\nabla}_M \times \bar{H}_\varphi) + \bar{\nabla}_M \times (\bar{\nabla}_M \times \bar{E}_\varphi) = \omega^2\mu\epsilon \bar{E}_M \ . \tag{3.14}$$

Thus, for azimuthally independent modes, the meridian plane field components are expressable in terms of the azimuthal components of $\bar{E}$ and $\bar{H}$. Two distinct mode types exist, one with vanishing $\bar{E}_\varphi$ the other with vanishing $\bar{H}_\varphi$.

Upon expanding Maxwell's equations (3.1a) and (3.1b), for azimuthally independent modes, two sets of relationships connecting the field components appear,

$$-\frac{\partial E_\varphi}{\partial z} = i\omega\mu H_r \tag{3.15a}$$

$$\frac{\partial E_r}{\partial z} - \frac{\partial E_z}{\partial r} = i\omega\mu H_\varphi \tag{3.15b}$$

$$\frac{1}{r}\frac{\partial(rE_\varphi)}{\partial r} = i\omega\mu H_z , \tag{3.15c}$$

and

$$\frac{\partial H_\varphi}{\partial z} = i\omega\epsilon E_r \tag{3.16a}$$

$$-\frac{\partial H_r}{\partial z} + \frac{\partial H_z}{\partial r} = i\omega\epsilon E_\varphi \tag{3.16b}$$

$$-\frac{1}{r}\frac{\partial(rH_\varphi)}{\partial r} = i\omega\epsilon E_z . \tag{3.16c}$$

The requirement for acceleration of particles (that the axial component of $\bar{E}$ not vanish) allows selection of those modes for which E_φ vanishes. In this event, H_r and H_z also vanish, cf. equations (3.15a), (3.15c), and (3.16b), and the vector wave equation (3.3) becomes a scalar wave equation

$$\frac{1}{r}\frac{\partial}{\partial r}\left(r\frac{\partial H_\varphi}{\partial r}\right) + \frac{\partial^2 H_\varphi}{\partial z^2} + \left(k^2 - \frac{1}{r^2}\right)H_\varphi = 0 , \tag{3.17}$$

where the eigenvalue k is related to the frequency ω and the wavelength λ by

$$k^2 = \omega^2\mu\epsilon = \left(\frac{2\pi}{\lambda}\right)^2 . \tag{3.18}$$

The boundary conditions which H_φ must obey is found from equation (3.4) with the assistance of equation (3.1b) and numerous vector identities as follows.

$$\epsilon \frac{\partial}{\partial t}(\bar{n}\times\bar{E}) = \bar{n}\times\frac{\partial \bar{D}}{\partial t} = \bar{n}\times(\bar{\nabla}\times\bar{H}_\varphi) = 0. \tag{3.19}$$

But, since $\bar{H}_\varphi = H_\varphi(r,z)\cdot\bar{u}_\varphi$,

$$\bar{\nabla}\times H_\varphi\bar{u}_\varphi = -\frac{\partial H_\varphi}{\partial z}\bar{u}_r + \frac{1}{r}\frac{\partial(rH_\varphi)}{\partial r}\bar{u}_z =$$

$$\frac{1}{r}\left[\frac{\partial(rH_\varphi)}{\partial r}\bar{u}_r + \frac{\partial(rH_\varphi)}{\partial z}\bar{u}_z\right]\times\bar{u}_\varphi = \frac{1}{r}\left[\bar{\nabla}(rH_\varphi)\times\bar{u}_\varphi\right]. \tag{3.20}$$

Thus it follows that equation (3.19) becomes

$$\bar{n}\times\frac{1}{r}\left[\bar{\nabla}(rH_\varphi)\times\bar{u}_\varphi\right] = (\bar{n}\cdot\bar{u}_\varphi)\frac{1}{r}\bar{\nabla}(rH_\varphi) - \frac{1}{r}\left[\bar{n}\cdot\bar{\nabla}(rH_\varphi)\right]\bar{u}_\varphi = 0. \tag{3.21}$$

And since $(\bar{n}\cdot\bar{u}_\varphi)$ vanishes, the boundary condition becomes

$$\bar{n}\cdot\bar{\nabla}(rH_\varphi) = \frac{\partial}{\partial n}(rH_\varphi) = 0. \tag{3.22}$$

In view of this boundary condition, it appears that the quantity rH_φ is of considerable interest. In fact, computer calculations are most easily done employing $F = rH_\varphi$ as the dependent variable rather than H_φ . The scalar wave equation (3.17) becomes, upon introduction of the quantity F,

$$\frac{\partial^2 F}{\partial r^2} - \frac{1}{r}\frac{\partial F}{\partial r} + \frac{\partial^2 F}{\partial z^2} + k^2 F = 0. \tag{3.23}$$

Henceforth, the primary concern of this endeavor will be directed toward the solutions of equation (3.23) valid in any meridian plane of a cavity of revolution and for azimuthally independent modes. Solutions will be sought for meridian plane geometries whose boundaries are piece-wise simply describable.

B. Exact Solutions of the Wave Equation

Exact solutions to the wave equations (3.17) and (3.23) can be found in the event that the boundaries of the geometry in question are coordinate surfaces in some coordinate system, and in the event that this coordinate system permits separation of variables.

A degenerate case of rotationally symmetric cavities for which an exact solution may be found is the hollow cylindrical cavity. Here the general solution of equation (3.17) is:

$$H_\varphi = H_0 \sum_{m=0}^{\infty} \sum_{n=1}^{\infty} \left[A_{nm} J_1(\chi_n r) + B_{nm} Y_1(\chi_n r) \right] e^{i\beta_m z}. \tag{3.24}$$

However, inclusion of the axis in the region of field penetration demands that, for all n and m, $B_{nm} = 0$. Furthermore, application of the boundary condition, equation (3.22), at $r = R$ (the outer radius of the cavity) demands that

$$J_0(\chi_n R) = 0, \qquad n = 1, 2, 3, \ldots \; . \tag{3.25}$$

Similarly, application of the boundary condition at $Z = \pm L/2$ (the ends of the cavity) demands that

$$\beta_m = \frac{2\pi m}{L}, \quad m = 0, 1, 2, 3, \ldots . \tag{3.26}$$

Hence the most general solution to the hollow cylindrical cavity problem is a double infinite sum of modes

$$H_\varphi = H_0 \sum_{m=0}^{\infty} \sum_{n=1}^{\infty} A_{nm} J_1(\chi_n r) e^{i\beta_m z}, \tag{3.27}$$

where the eigenvalue k for any n,m mode is given by

$$k_{nm}^2 = \chi_n^2 + \beta_m^2 = \chi_n^2 + \left(\frac{2\pi m}{L}\right)^2 . \tag{3.28}$$

Note that the modes discussed here are commonly known as the TM_{onm} modes. In particular, the lowest mode, i.e. that mode most easily excited in a hollow cylindrical cavity, is the TM_{010} mode

$$H_\varphi = H_0 J_1(\chi_1 r), \quad \text{where} \quad k_n^2 = \chi_1^2 = \left(\frac{2.405}{R}\right)^2 \tag{3.29}$$

In some instances, computer calculations are compared with results obtainable from equation (3.29) for the hollow cylindrical cavity.

C. Variational Principle Approach to Approximate Solutions of the Wave Equation

If the geometry in question does not permit separation of variables and satisfaction of the boundary conditions, exact

solutions to the scalar wave equations (3.17) and (3.23) can not be found. In this event, approximate solutions for both the eigenfunctions and the eigenvalues must suffice. As shall be seen, a convergent iterative process exists whereby a particular eigenfunction and the corresponding eigenvalue may be calculated. This is accomplished by alternately refining the field and a trial eigenvalue.

Consider, therefore, an arbitrary function (field distribution), existing in a cavity of revolution and satisfying the boundary condition (3.22), as a sum of orthonormal eigenfunctions of the cavity, i.e.

$$\phi = \sum_n A_n \phi_n \, . \tag{3.30}$$

If the eigenfunctions ϕ_n satisfy a scalar wave equation

$$\mathcal{L}\phi_n + k_n^2 \phi_n = 0 \, , \tag{3.31}$$

and also the boundary condition (3.22), it follows that equation (3.30) becomes

$$\mathcal{L}\phi = \mathcal{L}\sum_n A_n \phi_n = \sum_n A_n \mathcal{L}\phi_n = -\sum_n A_n k_n^2 \phi_n \, . \tag{3.32}$$

Upon forming the appropriate scalar product $\langle \phi, \mathcal{L}\phi \rangle$, and noting that if k_1 is the lowest of the eigenvalues, it follows that

$$\langle \phi, \mathcal{L}\phi \rangle = -\langle \sum_m A_m \phi_m, \sum_n A_n k_n^2 \phi_n \rangle$$

$$\geq -k_1^2 \langle \sum_m A_m \phi_m, \sum_n A_n \phi_n \rangle = -k_1^2 \langle \phi, \phi \rangle \, . \tag{3.33}$$

In the present instance, for TM modes in cavities of revolution, the operator $\mathcal{L}$ and the function ϕ may be identified via the scalar wave equation (3.23). The particular scalar product applicable for azimuthally independent modes in a cavity of revolution is indicated in MURA-481.[13] There results, therefore, from equation (3.33)

$$k_1^2 \leq -\frac{\langle \phi, \mathcal{L}\phi \rangle}{\langle \phi, \phi \rangle} = -\frac{\iint_S \frac{F}{r}\left[\frac{\partial^2 F}{\partial r^2} - \frac{1}{r}\frac{\partial F}{\partial r} + \frac{\partial^2 F}{\partial z^2}\right] dr\, dz}{\iint_S \frac{F^2}{r}\, dr\, dz} . \tag{3.34}$$

Thus, it is possible to find an upper bound of the lowest eigenvalue k_1 if the function in the domain of F is a linear combination of eigenfunctions.

It is also demonstrable that the variational principle leads to a convergent iterative process. Toward this end, suppose the function ϕ is expressable as the sum of a particular eigenfunction ϕ_n and a remainder, i.e.

$$\phi = \phi_n + \lambda \sum_m A_m \phi_m = \phi_n + \lambda \psi, \qquad m \neq n . \tag{3.35}$$

Thus, calculating the quantity

$$J(\lambda) = -\frac{\langle \phi, \mathcal{L}\phi \rangle}{\langle \phi, \phi \rangle} = -\frac{\langle \phi_n + \lambda\psi, \mathcal{L}\phi_n + \lambda\mathcal{L}\psi \rangle}{\langle \phi_n + \lambda\psi, \phi_n + \lambda\psi \rangle} , \tag{3.36}$$

via an expansion in λ such as

$$J(\lambda) = J(0) + \lambda\left(\frac{\partial J}{\partial \lambda}\right)_{\lambda=0} + \frac{\lambda^2}{2}\left(\frac{\partial^2 J}{\partial \lambda^2}\right)_{\lambda=0} + \cdots , \tag{3.37}$$

it follows that

$$J(0) = -\frac{\langle \phi_n, \mathcal{L}\phi_n \rangle}{\langle \phi_n, \phi_n \rangle} = +k_n^2 \frac{\langle \phi_n, \phi_n \rangle}{\langle \phi_n, \phi_n \rangle} = +k_n^2 , \tag{3.38}$$

and

$$\left(\frac{\partial J}{\partial \lambda}\right)_{\lambda=0} = -\frac{\langle \phi_n, \phi_n \rangle \left[\langle \phi_n, \mathcal{L}\psi \rangle + \langle \mathcal{L}\phi_n, \psi \rangle\right]}{\left[\langle \phi_n, \phi_n \rangle\right]^2} +$$

$$+ \frac{\langle \phi_n, \mathcal{L}\phi_n \rangle \left[\langle \phi_n, \psi \rangle + \langle \phi_n, \psi \rangle\right]}{\left[\langle \phi_n, \phi_n \rangle\right]^2} . \tag{3.39}$$

The numerator of equation (3.39) vanishes, providing the operator $\mathcal{L}$ is self adjoint, since in this event

$$\langle \phi_n, \mathcal{L}\psi \rangle = \langle \mathcal{L}\phi_n, \psi \rangle . \tag{3.40}$$

The numerator of equation (3.39) thus becomes

$$\begin{aligned} &\langle \phi_n, \phi_n \rangle \left[\langle \phi_n, \mathcal{L}\psi \rangle + \langle \mathcal{L}\phi_n, \psi \rangle\right] - \langle \phi_n, \mathcal{L}\phi_n \rangle \left[2 \langle \phi_n, \psi \rangle\right] \\ &= \langle \phi_n, \phi_n \rangle \left[2 \langle \mathcal{L}\phi_n, \psi \rangle\right] - \langle \phi_n, \mathcal{L}\phi_n \rangle \left[2 \langle \phi_n, \psi \rangle\right] \\ &= \langle \phi_n, \phi_n \rangle \left[-2k_n^2 \langle \phi_n, \psi \rangle\right] + k_n^2 \langle \phi_n, \phi_n \rangle \left[2 \langle \phi_n, \psi \rangle\right] = 0 . \end{aligned} \tag{3.41}$$

Combining this result with equations (3.37) and (3.38) yields

$$k_n^2 = J(\lambda) - \frac{\lambda^2}{2}\left(\frac{\partial^2 J}{\partial \lambda^2}\right)_{\lambda=0} - \cdots \quad . \tag{3.42}$$

It is thus seen that although the function ϕ may differ from an eigenfunction ϕ_n by an amount proportional to λ, the calculations of the quantity $J(\lambda)$ differs from the eigenvalue k_n^2 by an amount proportional to λ^2. Thus a convergent iterative process is realized if, alternately, the function ϕ is made to approximate an eigenfunction more closely, and an approximation to the eigenvalue is calculated via equation (3.36).

D. Approximate Solutions of the Wave Equation For Cavities Containing Square Cornered Drift-Tubes.

As indicated in some of the references listed in Chapter II, an approximate solution of the wave equation (3.23) may be obtained for linear-accelerator type cavities containing square cornered drift-tubes by making certain assumptions about the field components and the matching conditions at the junction of the two regions indicated in Figure 1. While this approach can produce some useful results, it is not applicable to cavities containing non-square cornered drift-tubes. Consequently, a alternative approach is desired.

With the advent of modern, high speed, digital computers, an alternate approach to the scalar wave equation (3.23) has

become possible. This is the finite-difference, mesh approach. The solution is relatively easily accomplished for the case of rectangularly piecewise continuous boundaries, but may be extended to other simply describable piecewise continuous boundaries.

To accomplish this finite-difference approach for a rectangularly bounded region, (see Figure 2) superimpose a finitely spaced square mesh upon the region such that the boundary of the region everywhere coincides with mesh lines. Then considering a typical mesh point (i,j) in the interior of the region, it follows that the one dimensional Taylor series expansions of the function F at this point are

$$F_{i,j+1} = F_{ij} + \frac{\partial F_{ij}}{\partial r} h + \frac{\partial^2 F_{ij}}{\partial r^2} \frac{h^2}{2} + \ldots + O(h^3) \tag{3.43}$$

$$F_{i,j-1} = F_{ij} - \frac{\partial F_{ij}}{\partial r} h + \frac{\partial^2 F_{ij}}{\partial r^2} \frac{h^2}{2} + \ldots - O(h^3) \tag{3.44}$$

$$F_{i+1,j} = F_{ij} + \frac{\partial F_{ij}}{\partial z} h + \frac{\partial^2 F_{ij}}{\partial z^2} \frac{h^2}{2} + \ldots + O(h^3) \tag{3.45}$$

$$F_{i-1,j} = F_{ij} - \frac{\partial F_{ij}}{\partial z} h + \frac{\partial^2 F_{ij}}{\partial z^2} \frac{h^2}{2} + \ldots - O(h^3) \tag{3.46}$$

where h is the mesh spacing and $O(h^3)$ is the order of maximum error size occuring due to neglection of further terms in the expansion. Adding and subtracting equations (3.43) and (3.44) yield in turn approximations for two derivatives

$$\frac{\partial^2 F_{ij}}{\partial r^2} = \frac{F_{i,j+1} + F_{i,j-1} - 2F_{ij}}{h^2} + O(h^2) \ , \tag{3.47}$$

$$\frac{\partial F_{ij}}{\partial r} = \frac{F_{i,j+1} - F_{i,j-1}}{2h} + O(h^2) \ . \tag{3.48}$$

Similarly, adding and subtracting equations (3.45) and (3.46) yield approximations for the other two derivatives

$$\frac{\partial^2 F_{ij}}{\partial z^2} = \frac{F_{i+1,j} + F_{i-1,j} - 2F_{ij}}{h^2} + O(h^2) \ , \tag{3.49}$$

$$\frac{\partial F_{ij}}{\partial z} = \frac{F_{i+1,j} - F_{i-1,j}}{2h} + O(h^2) \ . \tag{3.50}$$

Substitution of equations (3.47), (3.48), and (3.49), into the scalar wave equation (3.23) yields

$$F_{i,j+1}\left(1 - \frac{h}{2r_j}\right) + F_{i,j-1}\left(1 + \frac{h}{2r_j}\right) + F_{i+1,j} + F_{i-1,j}$$

$$+ (k^2h^2 - 4)F_{ij} + O(h^4) = 0 \ . \tag{3.51}$$

Note here that the resultant error is of maximum order h^4, and that as the number of points in the mesh increases, (i.e. as h decreases), the relative error vanishes.

In order to employ equation (3.51), omitting the term $O(h^4)$, k^2 must be known. Equation (3.34) gives an

approximation for the lowest eigenvalue for the cavity of revolution. Inserting equations (3.47), (3.48), and (3.49) yields

$$k_1^2 \approx -\frac{\sum_i \sum_j \frac{F_{ij}}{r_j}\left[F_{i,j+1}\left(1-\frac{h}{2r_j}\right)+F_{i,j-1}\left(1+\frac{h}{2r_j}\right)+F_{i+1,j}+F_{i-1,j}-4F_{ij}\right]}{\sum_i \sum_j \frac{(F_{ij})^2}{r_j} h^2}, \quad (3.52)$$

The application of the boundary condition, equation (3.22), may be accomplished, in the event that the point (i,j) falls on the boundary, by merely reflecting the function F at the boundary. For example, if the point (i,j) falls on the top boundary, (see Figure 2) the factor $F_{i,j+1}$ in equations (3.51) and (3.52) should be replaced by the factor $F_{i,j-1}$ after which combination of the remaining terms is permissible.

The relative ease of application of the boundary condition of $F = rH_\varphi$ is the principal reason for its employment as the dependent variable in the preceeding and following analysis.

Details on the iteration process employing equations (3.51) and (3.52) follow in Chapter IV.

E. Approximate Solutions of the Wave Equation for Cavities Containing Round and Elliptical Cornered Drift-Tubes

The aforementioned finite-difference method of solution of the scalar wave equation (3.23) may be extended and modified in order to handle drift-tube loaded cavities whose meridian plane cross-sections are bounded by circular and/or elliptical arcs

as in Figure 3.

To see how this can be accomplished, in the case of circular arc boundaries, let the scalar wave equation (3.23) be transformed into plane polar coordinates via the transformations,

$$r = r_c + \rho \sin\theta \,, \qquad z = z_c + \rho \cos\theta \,. \tag{3.53}$$

The result is such that

$$\frac{\partial^2 F}{\partial \rho^2} + \left[\frac{r_c}{\rho(r_c+\rho\sin\theta)}\right]\frac{\partial F}{\partial \rho} + \frac{1}{\rho^2}\frac{\partial^2 F}{\partial \theta^2} - \left[\frac{\cos\theta}{\rho(r_c+\rho\sin\theta)}\right]\frac{\partial F}{\partial \theta} + k^2 F = 0 \,. \tag{3.54}$$

Similarly the expression for the eigenvalue, equation (3.34) becomes

$$k_1^2 \leq - \frac{\iint_S \frac{F}{(r_c+\rho\sin\theta)}\left\{\frac{\partial^2 F}{\partial \rho^2} + \left[\frac{r_c}{\rho(r_c+\rho\sin\theta)}\right]\frac{\partial F}{\partial \rho} + \frac{1}{\rho^2}\frac{\partial^2 F}{\partial \theta^2} - \left[\frac{\cos\theta}{\rho(r_c+\rho\sin\theta)}\right]\frac{\partial F}{\partial \theta}\right\}\rho\, d\rho\, d\theta}{\iint_S \frac{F^2}{(r_c+\rho\sin\theta)}\rho\, d\rho\, d\theta} \,. \tag{3.55}$$

Now, establishing a plane polar mesh in the neighborhood of the circular arc boundary, such that the boundary coincides with a mesh line (see Figure 3), expanding the function F in Taylor series expansions, in the manner of equations (3.43), (3.44), (3.45), and (3.46), adding and subtracting the resulting expansions to find

approximations to the derivatives, and substituting these derivatives into equations (3.54) and (3.55) yields

$$F_{\ell+1,m}\left\{\frac{1}{h_\rho^2}+\frac{1}{2h_\rho}\left[\frac{r_c}{\rho(r_c+\rho\sin\theta)}\right]\right\}+F_{\ell-1,m}\left\{\frac{1}{h_\rho^2}-\frac{1}{2h_\rho}\left[\frac{r_c}{\rho(r_c+\rho\sin\theta)}\right]\right\}+$$

$$+F_{\ell,m+1}\left\{\frac{1}{h_\theta^2}-\frac{1}{2h_\theta}\left[\frac{\cos\theta}{(r_c+\rho\sin\theta)}\right]\right\}+F_{\ell,m-1}\left\{\frac{1}{h_\theta^2}+\frac{1}{2h_\theta}\left[\frac{\cos\theta}{(r_c+\rho\sin\theta)}\right]\right\}+$$

$$+F_{\ell,m}\left[-\frac{2}{h_\rho^2}-\frac{2}{h_\theta^2}+k^2\right]=0\,, \tag{3.56}$$

and

$$k^2\approx-\frac{\displaystyle\sum_\ell\sum_m\left\{\frac{F_{\ell,m}}{(r_c+\rho\sin\theta)}\cdot\left[F_{\ell+1,m}\left\{\frac{1}{h_\rho^2}+\frac{1}{2h_\rho}\left[\frac{r_c}{\rho(r_c+\rho\sin\theta)}\right]\right\}+F_{\ell-1,m}\left\{\frac{1}{h_\rho^2}-\frac{1}{2h_\rho}\cdot\left[\frac{r_c}{\rho(r_c+\rho\sin\theta)}\right]\right\}+F_{\ell,m+1}\left\{\frac{1}{h_\theta^2}-\frac{1}{2h_\theta}\left[\frac{\cos\theta}{(r_c+\rho\sin\theta)}\right]\right\}+F_{\ell,m-1}\left\{\frac{1}{h_\theta^2}+\frac{1}{2h_\theta}\left[\frac{\cos\theta}{(r_c+\rho\sin\theta)}\right]\right\}\right]h_\rho h_\theta\right\}}{\displaystyle\sum_\ell\sum_m\frac{F_{\ell,m}^2}{(r_c+\rho\sin\theta)}h_\rho h_\theta}\,. \tag{3.57}$$

Similarly for the case of elliptical arc boundaries the transformation equations are

$$r=r_c+c\sqrt{(1-\eta^2)(\xi^2-1)}\,,\qquad z=z_c+c\eta\xi\,, \tag{3.58}$$

where the quantity c is related to the eccentricity and the semi-major axis of the ellipse by

$$c = ae. \tag{3.59}$$

In this case the scalar wave equation (3.23) and the eigenvalue expression, equation (3.34), become

$$\frac{\partial^2 F}{\partial \xi^2}\left[\frac{(\xi^2-1)}{c^2(\xi^2-\eta^2)}\right] + \frac{\partial F}{\partial \xi}\left[\frac{\xi}{c^2(\xi^2-\eta^2)} - \frac{\xi\sqrt{(1-\eta^2)(\xi^2-1)}}{\left[r_c + c\sqrt{(1-\eta^2)(\xi^2-1)}\right]c(\xi^2-\eta^2)}\right] +$$

$$+ \frac{\partial^2 F}{\partial \eta^2}\left[\frac{(1-\eta^2)}{c^2(\xi^2-\eta^2)}\right] - \frac{\partial F}{\partial \eta}\left[\frac{\eta}{c^2(\xi^2-\eta^2)} - \frac{\eta\sqrt{(1-\eta^2)(\xi^2-1)}}{\left[r_c + c\sqrt{(1-\eta^2)(\xi^2-1)}\right]c(\xi^2-\eta^2)}\right] +$$

$$+ k^2 F = 0, \tag{3.60}$$

and

$$k_1^2 \approx - \frac{\displaystyle\iint_S \frac{F}{\left[r_c + c\sqrt{(1-\eta^2)(\xi^2-1)}\right]}\left\{\frac{\partial^2 F}{\partial \xi^2}\left[\frac{(\xi^2-1)}{c^2(\xi^2-\eta^2)}\right] + \frac{\partial F}{\partial \xi}\left[\frac{\xi}{c^2(\xi^2-\eta^2)} - \frac{\xi\sqrt{(1-\eta^2)(\xi^2-1)}}{\left[r_c + c\sqrt{(1-\eta^2)(\xi^2-1)}\right]c(\xi^2-\eta^2)}\right] + \right.}{}$$

$$\left. + \frac{\partial^2 F}{\partial \eta^2}\left[\frac{(1-\eta^2)}{c^2(\xi^2-\eta^2)}\right] - \frac{\partial F}{\partial \eta}\left[\frac{\eta}{c^2(\xi^2-\eta^2)} - \frac{\eta\sqrt{(1-\eta^2)(\xi^2-1)}}{\left[r_c + c\sqrt{(1-\eta^2)(\xi^2-1)}\right]c(\xi^2-\eta^2)}\right]\right\} \frac{c^2(\xi^2-\eta^2)}{\sqrt{(\xi^2-1)(1-\eta^2)}}\, d\xi\, d\eta}{\displaystyle\iint_S \frac{F^2}{\left[r_c + c\sqrt{(1-\eta^2)(\xi^2-1)}\right]} \cdot \frac{c^2(\xi^2-\eta^2)}{\sqrt{(\xi^2-1)(1-\eta^2)}}\, d\xi\, d\eta} \tag{3.61}$$

Furthermore, the finite difference approximations for equations (3.60) and (3.61) become, for a typical interior point (l,m),

$$F_{\ell+1,m}\left\{\frac{1}{h_\xi^2}+\frac{1}{2h_\xi}\left[\frac{\xi}{c\sqrt{(\xi^2-1)(1-\eta^2)}}-\frac{\xi}{r_c+c\sqrt{(\xi^2-1)(1-\eta^2)}}\right]\right\}+F_{\ell-1,m}\left\{\frac{1}{h_\xi^2}-\frac{1}{2h_\xi}\left[\frac{\xi}{c\sqrt{(\xi^2-1)(1-\eta^2)}}-\frac{\xi}{r_c+c\sqrt{(\xi^2-1)(1-\eta^2)}}\right]\right\}+$$

$$+F_{\ell,m+1}\left\{\frac{1}{h_\eta^2}-\frac{1}{2h_\eta}\left[\frac{\eta}{c\sqrt{(\xi^2-1)(1-\eta^2)}}-\frac{\eta}{r_c+c\sqrt{(\xi^2-1)(1-\eta^2)}}\right]\right\}+F_{\ell,m-1}\left\{\frac{1}{h_\eta^2}+\frac{1}{2h_\eta}\left[\frac{\eta}{c\sqrt{(\xi^2-1)(1-\eta^2)}}-\frac{\eta}{r_c+c\sqrt{(\xi^2-1)(1-\eta^2)}}\right]\right\}$$

$$+F_{\ell,m}\left[k^2-\left(\frac{2}{h_\xi^2}+\frac{2}{h_\eta^2}\right)\right]=0\,, \qquad (3.62)$$

and

$$k_1^2\approx-\frac{\displaystyle\sum_\ell\sum_m\left\{\frac{F_{\ell,m}}{\left[r_c+c\sqrt{(\xi^2-1)(1-\eta^2)}\right]}\cdot\left[F_{\ell+1,m}\left\{\frac{1}{h_\xi^2}+\frac{1}{2h_\xi}\left[\frac{\xi}{c\sqrt{(\xi^2-1)(1-\eta^2)}}-\frac{\xi}{r_c+c\sqrt{(\xi^2-1)(1-\eta^2)}}\right]\right\}+\right.\right.}{}$$

$$+F_{\ell-1,m}\left\{\frac{1}{h_\xi^2}-\frac{1}{2h_\xi}\left[\frac{\xi}{c\sqrt{(\xi^2-1)(1-\eta^2)}}-\frac{\xi}{r_c+c\sqrt{(\xi^2-1)(1-\eta^2)}}\right]\right\}+F_{\ell,m+1}\left\{\frac{1}{h_\eta^2}-\frac{1}{2h_\eta}\left[\frac{\eta}{c\sqrt{(\xi^2-1)(1-\eta^2)}}-\right.\right.$$

$$\left.\left.\left.\left.\frac{\eta}{r_c+c\sqrt{(\xi^2-1)(1-\eta^2)}}\right]\right\}+F_{\ell,m-1}\left\{\frac{1}{h_\eta^2}+\frac{1}{2h_\eta}\left[\frac{\eta}{c\sqrt{(\xi^2-1)(1-\eta^2)}}-\frac{\eta}{r_c+c\sqrt{(\xi^2-1)(1-\eta^2)}}\right]\right\}\right]\right\}}{\displaystyle\sum_\ell\sum_m\frac{F_{\ell m}^2}{\left[r_c+c\sqrt{(\xi^2-1)(1-\eta^2)}\right]}h_\xi h_\eta}\,. \qquad (3.63)$$

Analogous to the case of square mesh considerations, the boundary condition, equation (3.22), may be applied by merely

reflecting the function F at the boundary, e.g. replacing $F_{l-1,m}$ by $F_{l+1,m}$ if the point (l,m) falls on an appropriate boundary.

The method in which these expressions, equations (3.56), (3.57), (3.62), and (3.63), are used in the event of circular or elliptical arc boundaries is explained in Chapter IV which follows immediately.

IV. ITERATIVE SOLUTION OF FINITE-DIFFERENCE EQUATIONS

A. General Features

Two possible modes of operation of a low energy proton linear accelerator exist, one in which at any given instant, the axial E_z fields are in the same direction in each gap between drift-tubes, the other in which the axial E_z fields are oppositely directed in adjacent gaps. The first mode is commonly known as the 2π mode, the second as the π mode. In order for the π mode to exist, however, actual metallic walls must exist across the cavity at the midpoints of the drift-tubes. The present calculations are applicable to either the π mode or the 2π mode.

The present treatment of the cavity problem neglects non-uniform spacing between and unequal size of drift-tubes, i.e. effects caused by increasing particle velocity. The resulting periodicity of the drift-tubes permits the application of the boundary condition along transverse planes at $Z = 0, \pm L/2$, with a consequent confinement of attention to the region in the meridian plane ($0 \leq z \leq L/2$, $0 \leq r \leq R$).

In order to obtain a solution of the scalar wave equation (3.23) by instead employing the finite-difference equations (3.51) and (3.52), for a rectangularly bounded region, (see Figure 2), a two step iterative approach must be employed. An initial set of values of F is loaded onto the two dimensional mesh depicted

in Figure 2, such that one value of F is assigned to each point of intersection of a mesh line with another or with the boundary. Calculation of a trial eigenvalue, for the resulting linear combination of eigenfunctions, via equation (3.52) is carried out. With this trial value for the eigenvalue, the two dimensional array of F values is improved via formulas derived from equation (3.51) and explained below. Repetitive calculation of trial eigenvalues, improvement of the array of F values, etc., proceeds until a stationary condition is reached wherein no further significant change in either the array of F values or trial eigenfunction occurs.

With appropriate modifications, also expalined below, the cases of circular or elliptical cornered drift-tubes may by handled. In this case, however, interpolation between two overlapping but not necessarily coincident meshes must take place, with a considerable addition to the degree of complexity involved.

B. Mesh Refinement

Derivable from the finite difference equation (3.51), is the Liebmann four-point algorism:

$$F_{ij}^{n+1} - F_{ij}^{n} = \alpha\left\{F_{ij}^{n}\left(\frac{h^2 k^2}{4} - 1\right) + \frac{1}{4}\left[F_{i,j+1}^{n}\left(1 - \frac{h}{2r}\right) + F_{i,j-1}^{n+1}\left(1 + \frac{h}{2r}\right) + F_{i+1,j}^{n} + F_{i-1,j}^{n+1}\right]\right\}, \quad (4.1)$$

where it is assummed that the mesh is traversed in a regular manner, such that upon improving F_{ij}, the quantities $F_{i-1,j}$ and

$F_{i,j-1}$ have already been improved upon. Note here that the present traversal of the mesh is designated by the superscript n + 1, while the one just previously completed is designated by the superscript n.

Relationships similar to equation (4.1) can be derived for the plane polar coordinate mesh and the elliptical coordinate mesh, from equations (3.56) and (3.60), respectively. These are

$$F_{\ell,m}^{n+1}-F_{\ell,m}^{n}=\alpha\left\{F_{\ell,m}^{n}\left[\frac{k^2}{\left(\frac{2}{h_\rho^2}+\frac{2}{h_\theta^2}\right)}-1\right]+\frac{1}{\left(\frac{2}{h_\rho^2}+\frac{2}{h_\theta^2}\right)}\left[F_{\ell+1,m}^{n}\left\{\frac{1}{h_\rho^2}+\frac{1}{2h_\rho}\left[\frac{r_c}{\rho(r_c+\rho\sin\theta)}\right]\right\}+\right.\right.$$

$$+F_{\ell-1,m}^{n+1}\left\{\frac{1}{h_\rho^2}-\frac{1}{2h_\rho}\left[\frac{r_c}{\rho(r_c+\rho\sin\theta)}\right]\right\}+F_{\ell,m+1}^{n}\left\{\frac{1}{h_\theta^2}-\frac{1}{2h_\theta}\left[\frac{\cos\theta}{(r_c+\rho\sin\theta)}\right]\right\}+$$

$$\left.\left.+F_{\ell,m-1}^{n+1}\left\{\frac{1}{h_\theta^2}+\frac{1}{2h_\theta}\left[\frac{\cos\theta}{(r_c+\rho\sin\theta)}\right]\right\}\right]\right\}, \qquad (4.2)$$

and

$$F_{\ell,m}^{n+1}-F_{\ell,m}^{n}=\alpha\left\{F_{\ell,m}^{n}\left[\frac{k^2}{\left(\frac{2}{h_\xi^2}+\frac{2}{h_\eta^2}\right)}-1\right]+\frac{1}{\left(\frac{2}{h_\xi^2}+\frac{2}{h_\eta^2}\right)}\left[F_{\ell+1,m}^{n}\left\{\frac{1}{h_\xi^2}+\frac{1}{2h_\xi}\left[\frac{\xi}{c\sqrt{(\xi^2-1)(1-\eta^2)}}-\frac{\xi}{r_c+c\sqrt{(\xi^2-1)(1-\eta^2)}}\right]\right\}+\right.\right.$$

$$+F_{\ell-1,m}^{n+1}\left\{\frac{1}{h_\xi^2}-\frac{1}{2h_\xi}\left[\frac{\xi}{c\sqrt{(\xi^2-1)(1-\eta^2)}}-\frac{\xi}{r_c+c\sqrt{(\xi^2-1)(1-\eta^2)}}\right]\right\}+F_{\ell,m+1}^{n}\left\{\frac{1}{h_\eta^2}-\frac{1}{2h_\eta}\left[\frac{\eta}{c\sqrt{(\xi^2-1)(1-\eta^2)}}-\right.\right.$$

$$\left.\left.\left.\frac{\eta}{r_c+c\sqrt{(\xi^2-1)(1-\eta^2)}}\right]\right\}+F_{\ell,m-1}^{n+1}\left\{\frac{1}{h_\eta^2}+\frac{1}{2h_\eta}\left[\frac{\eta}{c\sqrt{(\xi^2-1)(1-\eta^2)}}-\frac{\eta}{r_c+c\sqrt{(\xi^2-1)(1-\eta^2)}}\right]\right\}\right]\right\}. \qquad (4.3)$$

Application of the boundary condition yields, for example, in the case of equation (4.1), on the top boundary where $F_{i,j+1}$

is to be replaced by $F_{i,j-1}$, the following reduction,

$$F_{ij}^{n+1} - F_{ij}^{n} = \alpha\left\{F_{ij}^{n}\left(\frac{h^2k^2}{4}-1\right) + \frac{1}{4}\left[2F_{i,j-1}^{n+1} + F_{i+1,j}^{n} + F_{i-1,j}^{n+1}\right]\right\} . \qquad (4.4)$$

Other reductions may be effected for other types of boundary points, both for the square mesh algorism (4.1) and the polar and elliptical mesh algorisms (4.2) and (4.3).

The factor α appearing in algorisms (4.1), (4.2), (4.3) and (4.4) is the over-relaxation factor. If $\alpha = 1$, these algorisms are rigorous. By judicious choice of $\alpha \geqslant 1$, accelerated convergence may be obtained. Although some attempts have been made to calculate the optimum value of α for algorisms derivable from Laplace's Equation, little information is available in connection with wave equations such as (3.23). An estimate of the order of magnitude of the optimum value of α for various numbers of mesh points is found experimentally to be:

No. of mesh points	55	200	700	1600	4300
Optimum α	1.40	1.63	1.79	1.82	1.85 .

C. Eigenvalue Calculation

Concurrently with or in juxtaposition to the process of mesh refinement, the continual improvement of the trial eigenvalue must occur. This requires the employment of relationships derivable from equations (3.52), (3.57), and (3.63), i.e. for a

rectangular mesh

$$\frac{k_1^2 h^2}{4} \simeq -\frac{\sum_i \sum_j \frac{F_{ij}^n}{r_j}\left\{\frac{1}{4}\left[F_{i,j+1}^n\left(1-\frac{h}{2r_j}\right)+F_{i,j-1}^n\left(1+\frac{h}{2r_j}\right)+F_{i+1,j}^n+F_{i-1,j}^n\right]-F_{ij}^n\right\}\Delta S_{ij}}{\sum_i \sum_j \frac{F_{ij}^2}{r_j}\Delta S_{ij}}, \quad (4.5)$$

for a circular mesh

$$\frac{k_1^2 h^2}{4} \simeq -\frac{\sum_l \sum_m \left\{\left[\frac{F_{l,m}^n}{\left(\frac{r_l}{h}+\frac{l}{h}\sin\theta\right)}\right]\cdot\frac{1}{4}\left[\frac{h^2}{h_\varphi^2}\left(F_{l+1,m}^n+F_{l-1,m}^n\right)+\frac{h^2}{h_\theta^2}\left(F_{l,m+1}^n+F_{l,m-1}^n\right)+\right.\right.}{\sum_l \sum_m \frac{(F_{l,m}^n)^2}{\left(\frac{r_l}{h}+\frac{l}{h}\sin\theta\right)}\Delta S_{l,m}}$$

$$\left.\left.+\left(\frac{h}{h_\varphi}\right)\frac{(F_{l+1,m}^n-F_{l-1,m}^n)}{2\left(\frac{r_l}{h}+\frac{l}{h}\sin\theta\right)}+\left(\frac{h}{h_\theta}\right)\frac{\cos\theta(F_{l,m-1}^n-F_{l,m+1}^n)}{2\left(\frac{r_l}{h}+\frac{l}{h}\sin\theta\right)}-2\left(\frac{h^2}{h_\varphi^2}+\frac{h^2}{h_\theta^2}\right)F_{l,m}^n\right]\right\}\Delta S_{l,m}, \quad (4.6)$$

etc. Note here that all F values from the nth traversal of the mesh must be used; consistency with the variational principle, equation (3.34), is thereby maintained.

In the event of circular or elliptical boundaries, the problem of the calculation of the trial eigenvalue becomes one of assigning proper areas to the various mesh points. Obviously an interior point of the square mesh requires area $\Delta S_{ij} = h^2$; a point on a rectilinear boundary requires $\Delta S_{ij} = \frac{1}{2}h^2$. For points near a curved boundary the assignment of areas may be accomplished by approximating (for this purpose alone) the curve by a polygonal line whereupon the area to be assigned is just that of a trapezoid of area

$$\Delta S_{ij} = \left(\delta+\frac{1}{2}\right)h^2, \quad (4.7)$$

where δ is the lesser of the two rectangular distances to the curve from the point (i,j).

In the event of circular or elliptical boundaries the use of relationships of the form of equation (4.6), etc. is restricted to the calculation of the braced quantities in the numerator. Interpolation between these quantities from the polar mesh points to a square mesh point allows assignment of areas according to (4.7).

In accordance with equations (3.35) and (3.42), it is found experimentally that the trial eigenvalue converges more rapidly than does the array of F values. Accordingly it is possible to decrease the frequency of calculation of the eigenvalue as the iteration process proceeds.

D. Interpolation Between Meshes

As indicated above, upon considering regions partially bounded by circular or elliptical arcs, it is often necessary to interpolate between two overlapping meshes. In order to be consistant with the amount of error outstanding in equation (3.51) for example, consider a two dimensional Taylor series expansion for the F function at a point (i,j) on the square mesh with respect to a point $(i+\alpha, j+\beta)$, $0 \leq \alpha, \beta \leq 1$. Dropping the subscripts (i,j) for convenience in favor of (0,0), it follows that

$$F_{00} = F_{\alpha\beta} - \alpha h \frac{\partial F_{\alpha\beta}}{\partial z} - \beta h \frac{\partial F_{\alpha\beta}}{\partial r} + \frac{\alpha^2 h^2}{2} \frac{\partial^2 F_{\alpha\beta}}{\partial z^2} + \alpha\beta h^2 \frac{\partial^2 F_{\alpha\beta}}{\partial z \partial r} + \frac{\beta^2 h^2}{2} \frac{\partial^2 F_{\alpha\beta}}{\partial r^2} + \ldots + O(h^3). \quad (4.8)$$

Similar expansions can be written for the points (0.1), (1.0), (1.1), and (A,B), the latter point being at a distance $\geqslant h$ from the point (α, β). Normally the point (A,B) should be chosen as the fifth nearest point to the point (α, β). Multiplying each of these equations by an unknown parameter λ_n it follows that upon combination

$$\left[-\lambda_1\alpha - \lambda_2\alpha + \lambda_3(1-\alpha) + \lambda_4(1-\alpha) + \lambda_5(A-\alpha)\right]h\cdot\frac{\partial F_{\alpha\beta}}{\partial z} +$$

$$+\left[-\lambda_1\beta + \lambda_2(1-\beta) - \lambda_3\beta + \lambda_4(1-\beta) + \lambda_5(B-\beta)\right]h\cdot\frac{\partial F_{\alpha\beta}}{\partial r} +$$

$$+\left[\lambda_1\frac{\alpha^2}{2} + \lambda_2\frac{\alpha^2}{2} + \lambda_3\frac{(1-\alpha)^2}{2} + \lambda_4\frac{(1-\alpha)^2}{2} + \lambda_5\frac{(A-\alpha)^2}{2}\right]h\cdot\frac{\partial^2 F_{\alpha\beta}}{\partial z^2} + \tag{4.9}$$

$$+\left[\lambda_1\alpha\beta - \lambda_2\alpha(1-\beta) - \lambda_3(1-\alpha)\beta + \lambda_4(1-\alpha)(1-\beta) + \lambda_5(A-\alpha)(B-\beta)\right]h^2\cdot\frac{\partial^2 F_{\alpha\beta}}{\partial r\,\partial z} +$$

$$+\left[\lambda_1\frac{\beta^2}{2} + \lambda_2\frac{(1-\beta)^2}{2} + \lambda_3\frac{\beta^2}{2} + \lambda_4\frac{(1-\beta)^2}{2} + \lambda_5\frac{(B-\beta)^2}{2}\right]h^2\cdot\frac{\partial^2 F_{\alpha\beta}}{\partial r^2} + k^2 F_{\alpha\beta} + O(h^3) =$$

$$\lambda_1\left[F_{00} - F_{\alpha\beta}\right] + \lambda_2\left[F_{01} - F_{\alpha\beta}\right] + \lambda_3\left[F_{10} - F_{\alpha\beta}\right] + \lambda_4\left[F_{11} - F_{\alpha\beta}\right] + \lambda_5\left[F_{AB} - F_{\alpha\beta}\right] + k^2 F_{\alpha\beta}\,.$$

Comparing and identifying the terms in equation (4.9) with those of equation (3.23), and omitting the error term $O(h^3)$ in (4.9), it follows that two conditions apply. These conditions

are

$$F_{\alpha\beta} = \frac{\lambda_1 F_{00} + \lambda_2 F_{01} + \lambda_3 F_{10} + \lambda_4 F_{11} + \lambda_5 F_{AB}}{\lambda_1 + \lambda_2 + \lambda_3 + \lambda_4 + \lambda_5 - k^2} , \qquad (4.10)$$

and

$$\begin{pmatrix} -\alpha h & -\alpha h & (1-\alpha)h & (1-\alpha)h & (A-\alpha)h \\ -\beta h & (1-\beta)h & -\beta h & (1-\beta)h & (B-\beta)h \\ \frac{\alpha^2}{2}h^2 & \frac{\alpha^2}{2}h^2 & \frac{(1-\alpha)^2}{2}h^2 & \frac{(1-\alpha)^2}{2}h^2 & \frac{(A-\alpha)^2}{2}h^2 \\ \alpha\beta h^2 & -\alpha(1-\beta)h^2 & -(1-\alpha)\beta h^2 & (1-\alpha)(1-\beta)h^2 & (A-\alpha)(B-\beta)h^2 \\ \frac{\beta^2}{2}h^2 & \frac{(1-\beta)^2}{2}h^2 & \frac{\beta^2}{2}h^2 & \frac{(1-\beta)^2}{2}h^2 & \frac{(B-\beta)^2}{2}h^2 \end{pmatrix} \begin{pmatrix} \lambda_1 \\ \lambda_2 \\ \lambda_3 \\ \lambda_4 \\ \lambda_5 \end{pmatrix} = \begin{pmatrix} 0 \\ -\frac{1}{r_\varphi} \\ 1 \\ 0 \\ 1 \end{pmatrix} . \qquad (4.11)$$

Solution of this matrix equation for λ_1 etc. allows the determination of $F_{\alpha\beta}$ via equation (4.10).

Results similar to equation (4.11) may be obtained for the value of $F_{\alpha\beta}$ within a polar mesh square. Note in this case (α, β) is an abbreviation for ($l + \alpha$, $m + \beta$). In this instance, being consistent with equation (3.54), it follows that equation (4.10) is valid providing the λ 's are determined

from

$$\begin{pmatrix} -\alpha h_\rho & -\alpha h_\rho & (1-\alpha)h_\rho & (1-\alpha)h_\rho & (A-\alpha)h_\rho \\ -\frac{\beta h_\theta}{\rho} & \frac{(1-\beta)h_\theta}{\rho} & -\frac{\beta h_\theta}{\rho} & \frac{(1-\beta)h_\theta}{\rho} & \frac{(B-\beta)h_\theta}{\rho} \\ \frac{\alpha^2 h_\rho^2}{2} & \frac{\alpha^2 h_\rho^2}{2} & \frac{(1-\alpha)^2 h_\rho^2}{2} & \frac{(1-\alpha)^2 h_\rho^2}{2} & \frac{(A-\alpha)^2 h_\rho^2}{2} \\ \frac{\alpha\beta h_\rho h_\theta}{\rho} & -\frac{\alpha(1-\beta)h_\rho h_\theta}{\rho} & -\frac{(1-\alpha)\beta h_\rho h_\theta}{\rho} & \frac{(1-\alpha)(1-\beta)h_\rho h_\theta}{\rho} & \frac{(A-\alpha)(B-\beta)h_\rho h_\theta}{\rho} \\ \frac{\beta^2 h_\theta^2}{2\rho^2} & \frac{(1-\beta)^2 h_\theta^2}{2\rho^2} & \frac{\beta^2 h_\theta^2}{2\rho^2} & \frac{(1-\beta)^2 h_\theta^2}{2\rho^2} & \frac{(B-\beta)^2 h_\theta^2}{2\rho^2} \end{pmatrix} \begin{pmatrix} \lambda_1 \\ \lambda_2 \\ \lambda_3 \\ \lambda_4 \\ \lambda_5 \end{pmatrix} = \begin{pmatrix} \frac{r_c/\rho}{(r_c+\rho\sin\theta)} \\ \frac{-\cos\theta}{\rho(r_c+\rho\sin\theta)} \\ 1 \\ 0 \\ \frac{1}{\rho^2} \end{pmatrix} . \tag{4.12}$$

In this manner values of F may be interpolated between the square and polar meshes. The same may be done with quantities calculated from the numerator of equation (4.6).

E. Normalization

In order to meaningfully compare eigenfunctions of two slightly dissimilar geometries, it is neccessary that uniform excitation of the cavity be maintained. A convienient quantity, to which the mesh values of F may be normalized, is the stored energy per unit valume. For the hollow cylindrical cavity this is known to be

$$W/V = \frac{1}{\pi R^2 L} \cdot \frac{\mu}{2} \iiint_V H_\varphi^2 dV = \frac{1}{\pi R^2 L} \cdot \frac{\mu}{2} \iiint_V H_0^2 J_1^2(kr) dV . \tag{4.13}$$

The boundary condition, equation (3.22), insures that

$$\frac{\partial}{\partial r}(rH_\varphi)\Big|_{r=R} = \frac{\partial}{\partial r}\Big[H_o r J_1(kr)\Big]_{r=R} = H_o R k J_o(kr) = 0 \ , \tag{4.14}$$

or $$J_o(kr) = 0 \ , \qquad kR = 2.405, \ldots \ . \tag{4.15}$$

Thus the stored energy per unit volume becomes

$$W/V = \frac{\mu}{2} \cdot H_o^2 J_1^2(kR) . \tag{4.16}$$

Now, since $F_o = RH_o$ via:

$$F = rH_\varphi = H_o r J_1(kr) = F_o \frac{r}{R} J_1(kr) \ , \tag{4.17}$$

it follows that

$$\frac{W}{V} R^2 = \frac{\mu}{2} F_o^2 J_1^2(kR) = 1.693 \times 10^{-7} F_o^2 \text{ joules/m} . \tag{4.18}$$

When calculating the eigenfunction for a hollow cylindrical cavity, it was decided to initially load the mesh with the function

$$F_{ij} = k r_j J_1(k r_j) \ , \tag{4.19}$$

so that $F_o = kR = 2.405$ amperes. Thus:

$$\frac{W}{V} R^2 = 9.791 \times 10^{-7} \text{ joules/m} . \tag{4.20}$$

This value of WR^2/V is maintained throughout all computer calculations.

It is also noted that the quantity WR^2/V is invariant to an expansion of the mesh, i.e. the inclusion of more mesh points in the same region. In finite mesh form, WR^2/V takes the form

$$\frac{W}{V}R^2 = \frac{\mu}{2}R^2 \frac{\sum_i \sum_j \left[F_{ij}^2/r_j\right] \Delta S_{ij}}{\sum_i \sum_j r_j \Delta S_{ij}} \sim F_o^2 . \tag{4.21}$$

Upon increasing the number of mesh points, letting γ be the ratio of increase in the number of points in either direction, and indicating the initial quantities by the subscript o, it follows that the conditions which hold are

$$\begin{gathered} i_o = \frac{1}{\gamma} i , \qquad j_o = \frac{1}{\gamma} j , \qquad (F_{ij})_o = F_{ij} , \\ (r_j)_o = r_j , \qquad (\Delta S_{ij})_o = \gamma^2 \Delta S_{ij} , \end{gathered} \tag{4.22}$$

and equation (4.21) becomes

$$\frac{\left(\frac{W}{V}R^2\right)}{\left(\frac{W}{V}R^2\right)_o} = \frac{(F_o^2)}{(F_o^2)_o} . \tag{4.23}$$

Moreover, if the value of F_o deviates from its prescribed value during the iteration process, renormalization becomes necessary. This may be done by comparing the final and initial values of WR^2/V and, in view of equation (4.21) dividing the F_{ij}'s by the square root of the ratio.

V. ASSOCIATED ELECTROMAGNETIC AND PARTICLE DYNAMICAL QUANTITIES

Some of the more important auxiliary quantities to consider in the optimization of linear accelerator parameters are defined as:

Stored Energy Per Unit Volume

$$\frac{W}{V} = \frac{\frac{\mu}{2}\iiint_V H_\varphi^2 dV}{\iiint_V dV} = \frac{\frac{\mu}{2}\iint_S \frac{E^2}{r} dS}{\iint_S r\, dS}, \tag{5.1}$$

where V = volume of cavity

and S = meridian half plane.

Power Lost to Cavity Walls

$$P_W = \frac{R_s}{2}\iint_{S'} H_\varphi^2 dS' = \pi R_s \oint \frac{E^2}{r} dl, \tag{5.2}$$

where S' = surface of cavity

and l = perimeter of meridian half plane.

Q Factor

$$Q = \frac{W}{P_W/\omega} = \omega \frac{\frac{\mu}{2}\iiint_V H_\varphi^2 dV}{\frac{R_s}{2}\iint_{S'} H_\varphi^2 dS'} = \frac{\omega\mu}{R_s} \frac{\iint_S \frac{E^2}{r} dS}{\oint \frac{E^2}{r} dl}, \tag{5.3}$$

where V, S', S, and l are as defined above.

Average Axial Accelerating Field

$$\mathcal{E}_0 = \frac{1}{L}\int_z E_z(0,z)\, dz = \frac{1}{\omega\epsilon L}\int_{-L/2}^{L/2} \left(\frac{1}{r}\frac{\partial F}{\partial r}\right)_{0,z} dz \,. \tag{5.4}$$

Shunt Impedance

$$Z_S = \frac{E_0^2}{P_W/L} = \frac{1}{\omega^2 \epsilon^2 \pi R_S L} \frac{\left[\int_{-L/2}^{L/2} \left(\frac{1}{r}\frac{\partial F}{\partial r}\right)_{0,z} dz\right]^2}{\oint \frac{F^2}{r} dl} . \tag{5.5}$$

Transit Time Factor

$$T = \frac{1}{L E_0} \int_z E_z(0,z) \cos\frac{2\pi z}{L} dz = \frac{1}{\omega \epsilon L E_0} \int_{-L/2}^{L/2} \left(\frac{1}{r}\frac{\partial F}{\partial r}\right)_{0,z} \cos\frac{2\pi z}{L} dz . \tag{5.6}$$

Note here that the quantity TE_0 is just the amount of energy gained per unit charge and per unit length by a synchronous axial particle.

Coupling Coefficient

$$S = \frac{1}{L^2 E_0} \int_z E_z(0,z)\, z \sin\frac{2\pi z}{L} dz = \frac{1}{\omega \epsilon L^2 E_0} \int_{-L/2}^{L/2} \left(\frac{1}{r}\frac{\partial F}{\partial r}\right)_{0,z} z \sin\frac{2\pi z}{L} dz . \tag{5.7}$$

Note that in order to calculate the last four of these quantities, the quantity $\left(\frac{1}{r}\frac{\partial F}{\partial r}\right)_{0,z}$ must be known. This may be determined by noting that, sinze E_z must remain finite everywhere, the function F must have an r, z dependence expressible at every point in the form

$$F(r,z) = b(z)\, r^2 + c(z)\, r^3 + \cdots . \tag{5.8}$$

Thus the required quantity for calculation of the latter four quantities above is

$$\left(\frac{1}{r}\frac{\partial F}{\partial r}\right)_{0,z} = 2\, b(z) . \tag{5.9}$$

The coefficients b(z), c(z), etc. in an expansion may of course be determined by a least-squares analysis of the mesh values of F.

VI. COMPUTATION PROGRAMS

A. Present Status

Results have been obtained from IBM 704 computer programs for the case of square ended drift-tubes. Programs have also been written to include drift-tubes with rounded corners and axial holes; these programs are still being checked. Also, the algorisms for the inclusion of elliptical boundaries have been derived.

B. Comparison of Results Obtained With Known Data

In connection with square ended drift-tubes, interpolation between curves given in Wilkins report[10] yields results which agree quite well with data calculated via the methods presented herein. Although the results calculated thus far are of limited extent, their apparent validity has warrented the extension of programming.

C. Future Aims and Additions

In addition to the inclusion of consideration of round cornered drift-tubes and axial holes into computer programs, and calculation of corresponding data, the inclusion of several other more sophisticated computer programs are of

interest. These include:

1. Allowance for elliptical cornered drift-tubes.
2. Construction of contour (equipotential) plots from mesh values of the eigenfunction.
3. Programmed modification of geometry so as to permit calculation of configurations whose eigenvalues are previously specified.
4. Calculation of the effect of non-uniform drift-tube sizes and spacings.
5. Investigation of other linear accelerator type cavities applicable to higher energy proton linear accelerators, e.g. disk loaded wave quide type structures, etc.
6. Calculation of the quantities listed in Chapter V so as to assist with the choice of the optimum geometrical configuration and the final design parameters.

VII. CONCLUSION

Calculation of eigenfunctions and eigenvalues for cavities of revolution via solution of finite difference equations have been carried out for cavities containing square ended drift-tubes. These calculations have been done with the aid of an IBM 704 computer program. Programs for consideration of round corner drift-tubes with axial holes have also been written. These and similar other programs, yet to be written, will provide data for the design of a 200 Mev proton linear accelerator.

REFERENCES

[1] Hansen, W.W., "On the Resonant Frequency of Closed Concentric Lines," Journal of Applied Physics, X, (1939), 38.

[2] Hahn, W.C., "New Method for the Calculation of Cavity Resonators," Journal of Applied Physics, XII, (1941), 62.

[3] Brillouin, L., Wave Propagation in Periodic Structures, McGraw-Hill, Inc., New York, 1946.

[4] Brillouin, L., "Wave Guides For Slow Waves," Journal of Applied Physics, XIX, (1948), 1023.

[5] Chu, E.L., and W.W. Hansen, "Theory of Disk-Loaded Wave Guides," Journal of Applied Physics, XVIII, (1947), 996.

[6] Walkinshaw, W., "Note on 'Wave Guides For Slow Waves,'" Journal of Applied Physics, XX, (1949), 634.

[7] Walkinshaw, W., and J.S. Bell, "Review of Theory of Metal Loaded Linear Accelerator," A.E.R.E. Report G/R 675, 1951.

[8] Bell, J.S., "A Variational Approach to Disk Loaded Waveguides," A.E.R.E. Report G/R 680, 1951.

[9] Walkinshaw, W., C.S. Sabel, and S. Outram, "Shunt Impendence Calculations For Proton Linear Accelerators" - Parts I and II, A.E.R.E. Reports T/M 104 and T/M 105, 1954.

[10] Wilkins, J.J., "Design Notes on Resonators For Proton Linear Accelerators," A.E.R.E. Report GP/R 1613, 1955.

[11] Christofilos, N.C., "Method of Computation of Drift-Tubes Shapes," Cern Symposium on High Energy Accelerators and Pion Physics Proceedings, I, (1956), 176.

[12]Taylor, R., "Calculation of Drift-Tube Dimensions in Linac Injector for the 7 Gev Harwell Proton Synchrotron," A.E.R.E. Report R3012, 1959.

[13]Van Bladel, J., "Sets of Eigenvectors for Volumes of Revolution," MURA Report 481, 1959.

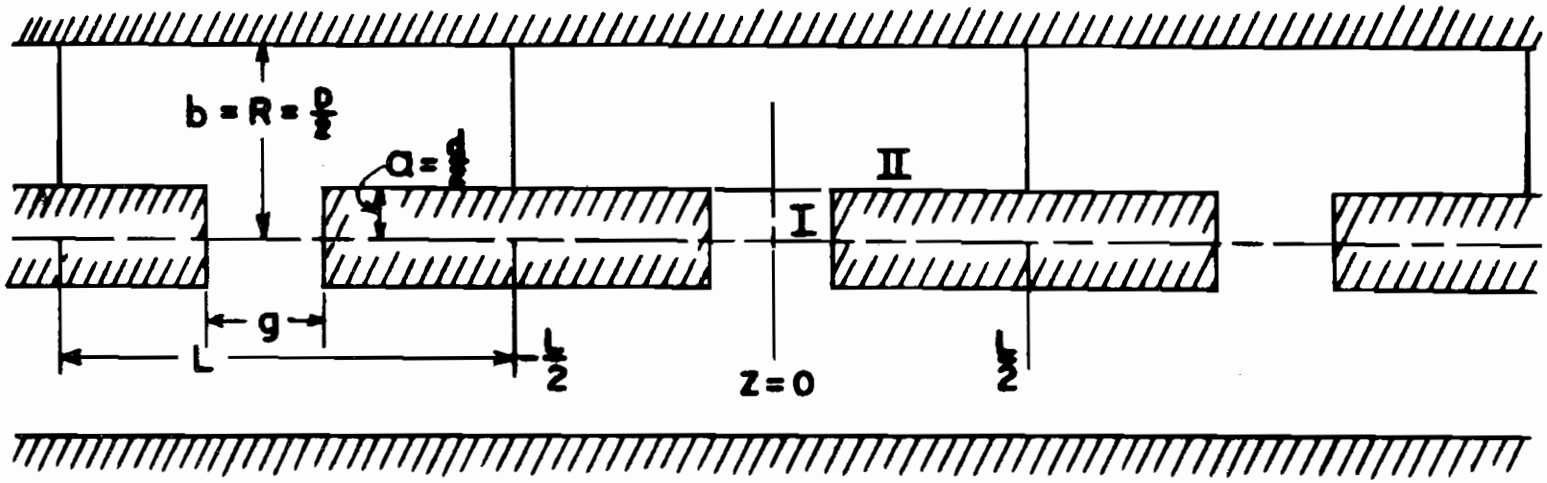

F I G U R E 1

PROTON LINEAR ACCELERATOR CAVITIES CONTAINING

Square-Ended Drift-Tubes

Region I: Gap Region Region II: Coaxial Line Region

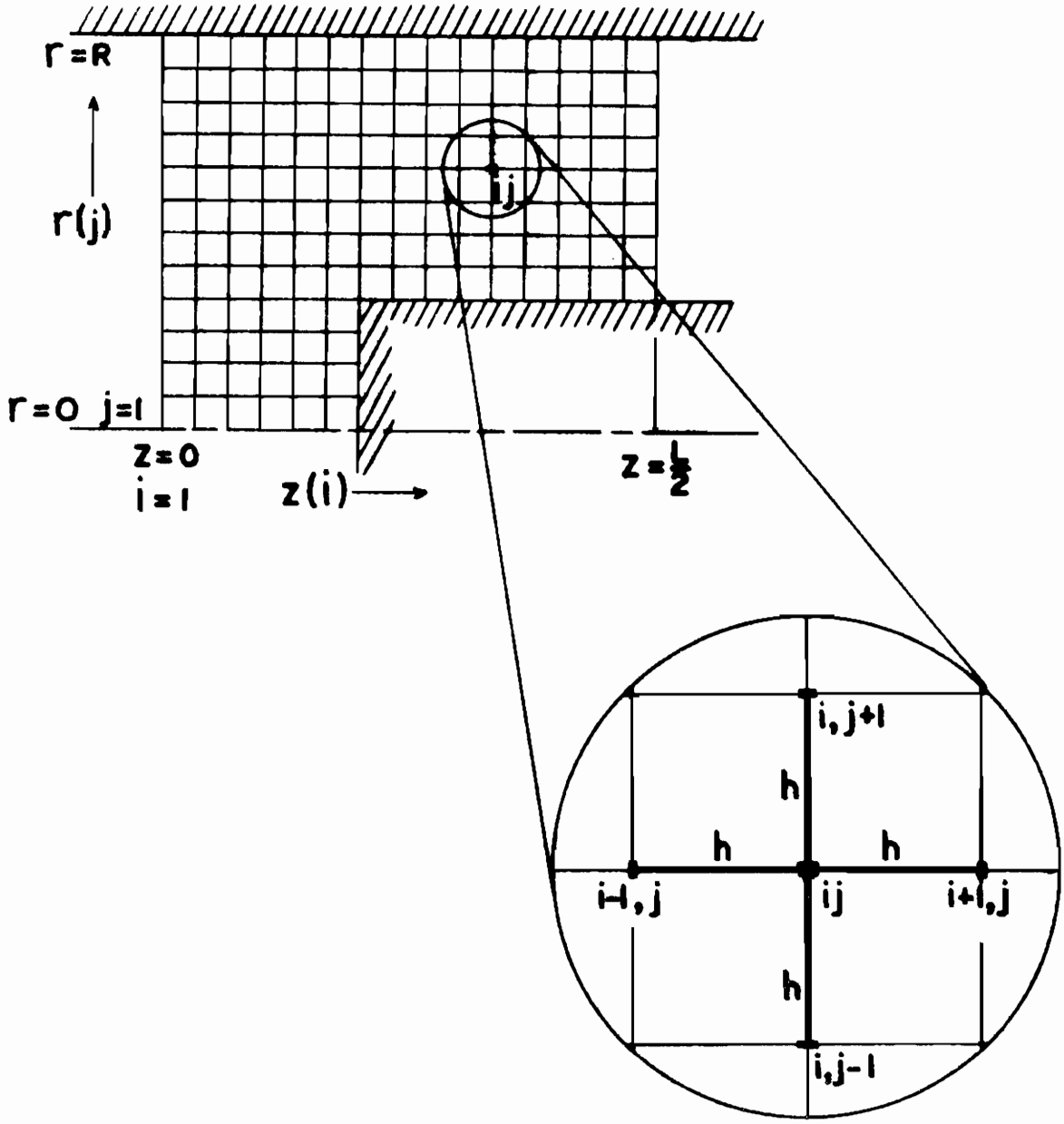

F I G U R E 2

A Finite Square Mesh Superimposed Upon

A Rectangularly Bounded Region

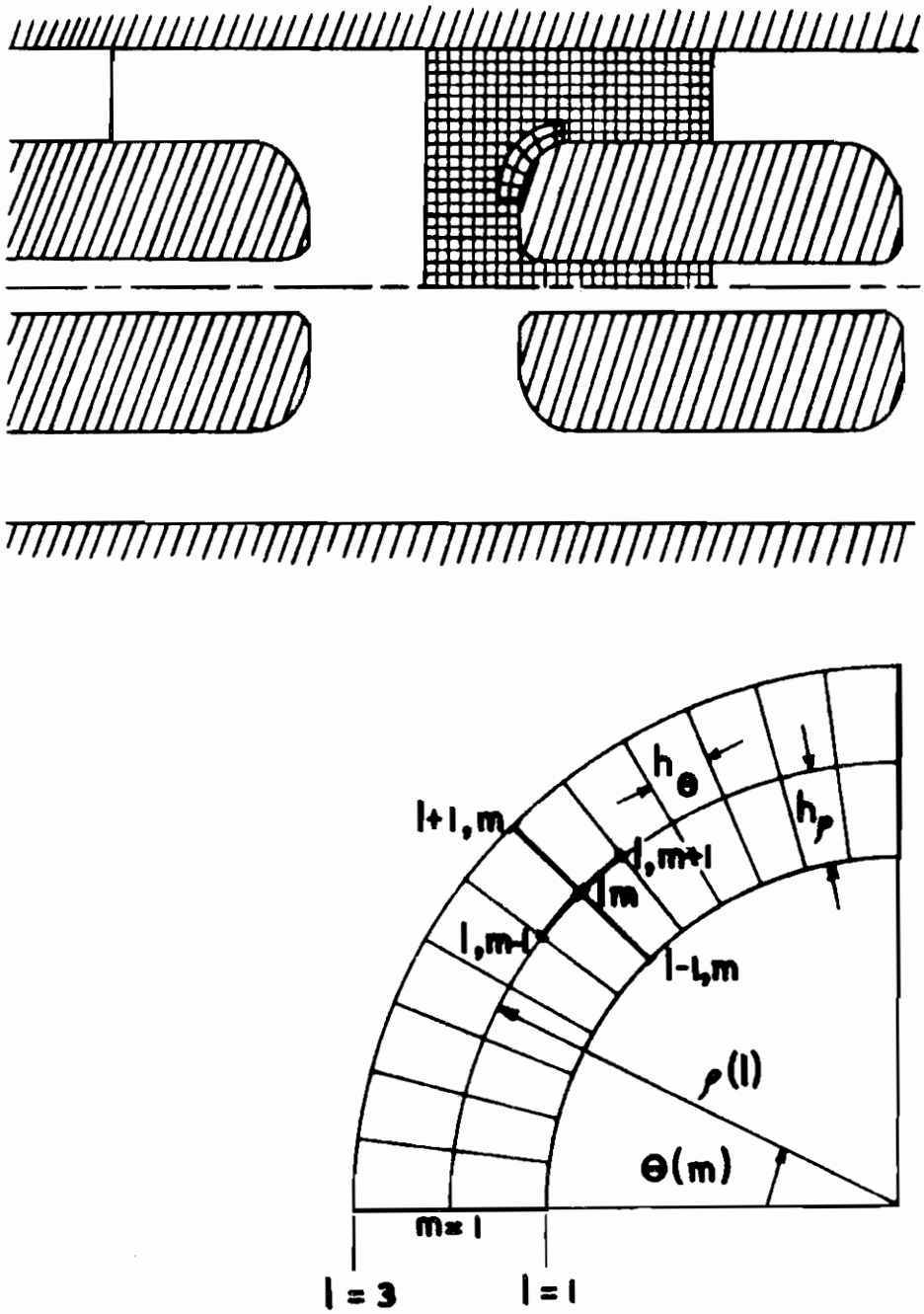

F I G U R E 3

Overlaping Square and Polar (Circular) Meshes

In The Neighborhood of A Circular Boundary

LEGAL NOTICE

This report was prepared as an account of Government sponsored work. Neither the United States, nor the Commission, nor any person acting on behalf of the Commission:

A. Makes any warranty or representation, expressed or implied, with respect to the accuracy, completeness, or usefulness of the information contained in this report, or that the use of any information, apparatus, method, or process disclosed in this report may not infringe privately owned rights; or

B. Assumes any liabilities with respect to the use of, or for damages resulting from the use of any information, apparatus, method, or process disclosed in this report.

As used in the above, "person acting on behalf of the Commission" includes any employee or contractor of the Commission, or employee of such contractor, to the extent that such employee or contractor of the Commission, or employee of such contractor prepares, disseminates, or provides access to, any information pursuant to his employment or contract with the Commission, or his employment with such contractor.

Printed in USA. Price $0.50. Available from the

Office of Technical Services
U. S. Department of Commerce
Washington 25, D. C.